CHEMPHYSCHEM

DOI: 10.1002/cphc.200600658

Comparison of Thermodynamic Properties of Coarse-Grained and Atomic-Level Simulation Models

Riccardo Baron,[a] Daniel Trzesniak,[a] Alex H. de Vries,[a, b] Andreas Elsener,[a] Siewert J. Marrink,[b] and Wilfred F. van Gunsteren*[a]

Thermodynamic data are often used to calibrate or test atomic-level (AL) force fields for molecular dynamics (MD) simulations. In contrast, the majority of coarse-grained (CG) force fields do not rely extensively on thermodynamic quantities. Recently, a CG force field for lipids, hydrocarbons, ions, and water,[1] in which approximately four non-hydrogen atoms are mapped onto one interaction site, has been proposed and applied to study various aspects of lipid systems. To date, no extensive investigation of its capability to describe solvation thermodynamics has been undertaken. In the present study, a detailed picture of vaporization, solvation, and phase-partitioning thermodynamics for liquid hydrocarbons and water was obtained at CG and AL resolutions, in order to compare the two types of models and evaluate their ability to describe thermodynamic properties in the temperature range between 263 and 343 K. Both CG and AL models capture the experimental dependence of the thermodynamic properties on the temperature, albeit a systematically weaker dependence is found for the CG model. Moreover, deviations are found for solvation thermodynamics and for the corresponding enthalpy–entropy compensation for the CG model. Particularly water/oil repulsion seems to be overestimated. However, the results suggest that the thermodynamic properties considered should be reproducible by a CG model provided it is reparametrized on the basis of these liquid-phase properties.

Introduction

In recent years there has been constant growing interest in the development of simple coarse-grained (CG) models for a variety of polymers,[2–4] lipids and surfactants,[1,5–11] and proteins,[12–14] which concentrates on computer simulations of longer time and larger size scales at the expense of lower resolution representations of structural and dynamical properties. Different from the classical atomic-level (AL) representations,[15–17] these models and their correspondingly simplified force fields consist of beads (also called superatoms or interaction sites with mass) representing groups of atoms, monomers, or even several monomer units. The beads interact through effective interaction functions that take into account the response of the omitted degrees of freedom effectively in an average way. How effectively a CG model performs mainly depends on the chosen coarse-graining procedure: i) the model resolution (how many AL particles per CG bead), ii) the mapping procedure (how the bead positions are defined as a function of the AL particle coordinates), iii) the potential energy function entering the CG Hamiltonian, and iv) the experimental and/or AL simulation properties against which the CG model is calibrated.

The available CG force fields have not been parameterized by making extensive use of thermodynamic quantities measured for the particular compounds. Yet hydration free energies (ΔF_{hyd}), vaporization enthalpies (ΔH_{vap}), and liquid-phase densities (ρ) of small organic compounds can be employed to calibrate AL biomolecular force fields.[19–21] Solvation thermodynamics of small compounds give an insight into physicochemical equilibria.[22–25] The extent to which a compound partitions between two separate environments (e.g. an aqueous phase and an organic phase) is a fundamental quantity for a variety of chemical and biochemical phenomena. Considerable effort has been made in the past decades towards the tabulation of experimentally determined partition coefficients and the development of theoretical models to predict partition coefficients.[26–28] These data are generally based on empirically derived contributions defined per functional group of atoms in a coarse-grained fashion. They have been shown to supply accurate thermodynamic descriptions of partitioning in the special case of homogeneous systems. However, they generally fail in those cases where the environment cannot be approximated

[a] Dr. R. Baron, D. Trzesniak, Dr. A. H. de Vries, A. Elsener, Prof. Dr. W. F. van Gunsteren
Laboratorium für Physikalische Chemie
ETH, Swiss Federal Institute of Technology Zürich
8093 Zürich (Switzerland)
Fax: (+41) 44-632-1039
E-mail: wfvgn@igc.phys.chem.ethz.ch

[b] Dr. A. H. de Vries, Prof. Dr. S. J. Marrink
Department of Biophysical Chemistry
Groningen Biomolecular Sciences and Biotechnology Institute
University of Groningen
Nijenborgh 4, 9747 AG, Groningen (The Netherlands)

Supporting information for this article is available on the WWW under http://www.chemphyschem.org or from the author.

WILEY InterScience DISCOVER SOMETHING GREAT

© 2007 Wiley-VCH Verlag GmbH & Co. KGaA, Weinheim

as a continuum, which is often the case of interest in biological systems.

The subject of the present article is the vaporization, solvation, and water/oil partitioning thermodynamics of aliphatic hydrocarbons studied from MD simulations with the recently developed CG force field by Marrink et al.,[1] an off-lattice model developed on the idea of the first model proposed by Smit et al.,[5] applied to study a water/oil interface in the presence of micelles[5] and surfactant self-assembly. This simple model maps approximately four non-hydrogen atoms to one interaction site and has been designed to simulate lipid aggregates in water. The corresponding water beads obey the same mapping scheme, each bead representing a cluster of four water molecules. The precise mapping depends on the number of atoms of a molecule; it need not be strictly 1 to 4. When comparing properties with experimental data, it should be kept in mind that a CG model represents more than one mapping. In order to keep the model as simple as possible, the CG force field was based on only five types of pair-interaction parameters and equal bead masses (72 u).[1] This same CG force field has been applied to study several properties of lipid systems,[1,29–32] but it has not yet been validated concerning the reproduction of experimental and/or theoretical thermodynamic quantities, except for free energies of partitioning of water beads in hexadecane, and of butane in water.[1] Recently, two comparative studies based on configurational entropy estimates for liquid hydrocarbons[33] and pure and mixed lipid bilayers[32] reported good correspondence between this CG model and the AL GROMOS model in terms of sampled configurational space and average structures. The loss in configurational entropy due to the coarse graining was also estimated.[32,33] In the present work, we focus on validation of the thermodynamic properties of the CG model for physicochemical equilibria (i.e. water/oil phase partition) of importance in biological processes. Partition coefficients are directly related to the differences in free energy and entropy of the compound in the two different environments.[34–36]

Free-energy differences may be calculated via thermodynamic integration (TI),[37–46] particle insertion,[47–49] or finite-temperature differences.[50] In practice, such free-energy calculations for small compounds are highly accurate within the force field and simulation methodology employed. In principle, the estimation of entropy differences by using these approaches is also possible. However, it requires appropriate sampling of the regions of phase space where the Hamiltonians corresponding to the two states of the system differ significantly, and can thus be a difficult task in practice.[44,51]

Four thermodynamic quantities were calculated for water and the set of alkanes considered: i) their vaporization enthalpies (ΔH_{vap}), ii) their excess Helmholtz free energies (ΔF_{exc}), iii) their hydration free energies (ΔF_{hyd}), and iv) the free energy (ΔF_{solv}) of solvating water into the corresponding liquid hydrocarbons. From the difference of these quantities it is possible to derive the corresponding free energies of partitioning which provide a thermodynamic description of the water/oil phase separation. More than two thousand simulations (corresponding to a total simulation time of more than 50 μs) were performed to this end. In order to estimate the change of entropy upon solvation we made use of a finite-difference approach using simulations performed at different temperatures, assuming a constant heat capacity over the temperature range considered. The set of hydrocarbons has been chosen with an eye to the occurrence of aliphatic fragments in lipids of biological interest. It has been limited to *n*-alkanes of chain length up to hexadecane (four corresponding CG beads). We report the results of two versions of the CG potential energy function: i) the version used in the parameterization applied with the GROMACS simulation software, and ii) a slightly modified version used with the GROMOS05 simulation software. Both potential energy functions are of the shifted/switched type, enforcing smooth decay to zero of potential energy and force at the cutoff distance. The two forms match closely in the region around the minimum of the potential energy. A discussion on the shifting and switching potential energy terms used in combination with the GROMACS[52] and GROMOS05[53] simulation programs is presented in the Appendix.

Results and Discussion

Liquid and Vaporization Properties at CG and AL Resolutions

Table 1 displays the physical properties for water (wt) and for the aliphatic hydrocarbons *n*-butane (C4), *n*-octane (C8), *n*-dodecane (C12), and *n*-hexadecane (C16). Experimental and calculated values from MD simulations at 303 K based on different model resolutions are reported for the average liquid density (ρ), the self-diffusion coefficients (D), and the enthalpies of vaporization (ΔH_{vap}).

A comparison of average liquid densities shows a good correspondence between AL (ρ^{AL}) and experimental (ρ^{exp}) values. For water both CG models (see Figure 7, Appendix) yield good agreement with experiment. For the alkanes, when using the real masses of the beads (56–58 u) instead of the model one (72 u), larger deviations (up to 19%) are found between both CG (ρ^{CG}) results and ρ^{exp} values. These deviations decrease with increasing chain length of the alkanes. The difference in density due to the different treatments of nonbonded interactions in the two CG models is at most 3%. Details on the different implementation of the nonbonded potential energy terms in GROMACS and GROMOS05 are discussed in the Appendix.

Figure 1 shows structural properties of liquid C16 for the AL and CG models at 323 K using particle–particle radial distribution functions: i) for the original CG model[1] using the GROMACS nonbonded interaction term[52] (code: rdf 1), ii) for the same CG model[1] treating the nonbonded interactions as in the GROMOS05 nonbonded interaction term[53] (code: rdf 2), iii) for the AL model (code: rdf 3), and iv) for the centers of mass of the CG fragments (MAP) mapped from the AL model with a 4:1 mapping scheme (code: rdf 4).[33] The CG models evidence stronger ordering than the AL model, especially in the first coordination shell. However, the number of particles in this first shell [about 6 for the (mapped) CG models; about 24 for the AL model] is similar in the four cases, as inferred

 © 2007 Wiley-VCH Verlag GmbH & Co. KGaA, Weinheim

Table 1. Physical properties of the CG model compared to experiment and to AL simulations. Liquid densities, self-diffusion coefficients, and enthalpies of vaporization from experiments (ρ^{exp};D^{exp};ΔH_{vap}^{exp}), using the CG model (ρ^{CG};D^{CG};ΔH_{vap}^{CG}), and the GROMOS 45A3 AL force field (ρ^{AL};D^{AL};ΔH_{vap}^{AL}). Values from simulations are reported followed by the corresponding average temperatures and their standard deviations.

	ρ^{exp} [a]	ρ^{CG} [b]	ρ^{CG} [c]	ρ^{AL} [d]	D^{exp} [e]	D^{CG} [b]	D^{CG} [c]	D^{AL} [d]	ΔH_{vap}^{exp} [f]	ΔH_{vap}^{CG} [b]	$\langle T\rangle$	ΔH_{vap}^{CG} [c]	$\langle T\rangle$	ΔH_{vap}^{AL} [d]	$\langle T\rangle$
	[g cm^{-3}]					[10^{-9} m^2 s^{-1}]			[kJ mol^{-1}]	[kJ mol^{-1}]	[K]	[kJ mol^{-1}]	[K]	[kJ mol^{-1}]	[K]
wt	0.99	0.99	0.96	0.97	2.4	2.0	2.0	4.2	43.9	29.0 ± 0.1	303 ± 1	30.1 ± 0.1	301 ± 1	42.0 ± 0.1	302 ± 3
C4	0.58	0.68	0.69	0.57	> 5.0	1.9	1.8	5.2	21.0	13.5 ± 0.1	303 ± 1	15.4 ± 0.1	302 ± 1	19.7 ± 0.3	302 ± 3
C8	0.70	0.78	0.78	0.70	2.0	0.6	0.5	3.3	41.5	31.9 ± 0.2	303 ± 1	30.5 ± 0.2	302 ± 1	39.6 ± 0.4	302 ± 3
C12	0.75	0.80	0.81	0.74	–	0.3	0.2	1.6	61.5	45.1 ± 0.2	303 ± 1	44.6 ± 0.2	302 ± 1	60.4 ± 0.4	302 ± 3
C16	0.77	0.81	0.83	0.77	–	0.2	0.2	0.9	81.3	64.5 ± 0.2	303 ± 1	60.3 ± 0.2	301 ± 1	80.4 ± 0.7	302 ± 3

[a] Values measured at 293 K from Lide[54] [b] This study, using the GROMACS setup of ref. [1], a 20 fs time step, $r_l = 0.9$ nm and $r_c = 1.2$ nm; effective self-diffusion coefficients in the case of water. [c] This study, using the GROMOS05 Lennard–Jones potential energy term, a 20 fs time step, $r_l = 0.0$ nm, and $r_c = 1.4$ nm; self-diffusion coefficients are reported relative to the experimental value of liquid water, as in ref. [1]. [d] This study, from 1 ns GROMOS 45A3 AL simulations at $T = 303$ K using a 2 fs time step. [e] Water, extrapolated to 303 K from Krynicki et al.[55] hydrocarbons: extrapolated to 303 K from Douglass and Mccall[56] [f] Lide,[54] Values were measured at 298 K, but at 321 K for C16.

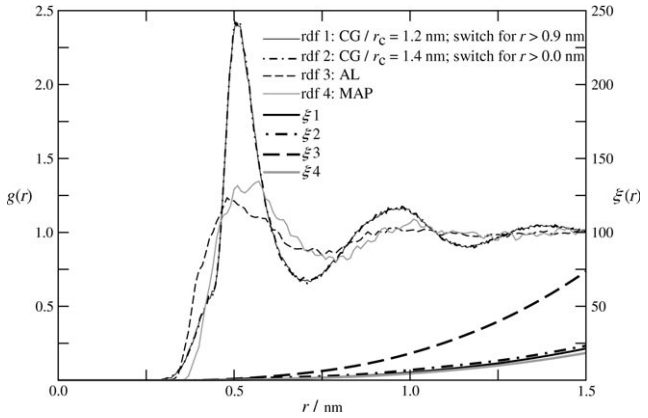

Figure 1. Radial distribution functions $g(r)$ and their integrals $\xi(r)$ from (CG: 15 ns; AL: 6 ns) simulations of liquid C16 at 323 K. For the CG model they are from calculations as in Marrink et al.[1] (——; 20 fs time step, $r_l = 0.9$ nm and $r_c = 1.2$ nm) or as described in this work (–•–•; 20 fs time step, $r_l = 0.0$ nm and $r_c = 1.4$ nm). For the AL model they are calculated by using united atoms (– – –) or the corresponding mapped beads (MAP; ——). The functions are calculated for the terminal particles of the chains (rdf, thin lines) taking into account all united atoms, mapped beads, or beads excluding intramolecular pairs. The corresponding running integrals $\xi(r)$ of $4\pi r^2 \rho g(r)$ are also shown (corresponding thick lines).

from the integral ξ over the radial distribution function. In general the structure of CG C16 liquids is similar for the two treatments of nonbonded interaction.

Table 1 also reports the self-diffusion coefficients from the same simulations, from previous work[1] and (whenever available) from experiment.[54,55] A direct comparison between absolute CG (D^{CG}) and AL (D^{AL}) coefficients is not possible, because the diffusion of simplified beads representing a water tetramer or groups of aliphatic CH_n groups is intrinsically different, due to smoother potentials and a reduced number of interactions. As previously suggested,[1] D^{CG} values are effective values in the case of CG water diffusion (i.e. scaled to the diffusion of 4 SPC water molecules). In an attempt to compare the AL model diffusion with that of the CG model, we calculated the self-diffusion coefficient of a water tetramer in SPC water and in SPC tetramer water at the AL level. We find a self-diffusion coefficient for a SPC water tetramer in SPC water of 4.0×10^{-9} m^2 s^{-1}, a value only slightly smaller than the SPC one of 4.2×10^{-9} m^2 s^{-1}. Interestingly, a value of 2.7×10^{-9} m^2 s^{-1} is found for the self-diffusion coefficient of the same SPC tetramer in a solution of SPC tetramers, which is closer to the D^{CG} value of 2.0×10^{-9} m^2 s^{-1}. The trend in the results for different alkane chain lengths agrees with that for the AL model.

Vaporization enthalpies were calculated from CG (ΔH_{vap}^{CG}) and AL (ΔH_{vap}^{AL}) simulations at 303 K. In this case, corresponding CG values are not available from Marrink et al.,[1] with the only exception of C16, for which a value of 66 kJ mol^{-1} was estimated.[33] As expected, ΔH_{vap}^{AL} values at 303 K are in good agreement with experiment and with previous calculations[20] at 298 K. For the CG water model, in which a CG bead represents a water tetramer, the energy needed to separate the tetramer into four (non-interacting) water molecules must be added to ΔH_{vap}^{CG} when comparing with ΔH_{vap}^{exp}. This tetramer energy is estimated to be 16 kJ mol^{-1} using the AL model, giving a value for ΔH_{vap}^{CG} of 46 kJ mol^{-1}, which is close to the experimental value. For the alkanes a large deviation from experiment (up to 36% for C4) is observed. The ΔH_{vap}^{CG} values deviate by up to 31% from the corresponding ΔH_{vap}^{AL} results. The CG model systematically underestimates the heat of vaporization. All (free) energy values investigated are found to be rather similar between the two different nonbonded interaction treatments.

Helmholtz and Solvation Free Energies of Alkanes at CG and AL Resolutions

Table 2 summarizes the Helmholtz excess free energies for the alkanes at different model resolutions (ΔF_{exc}^{CG} and ΔF_{exc}^{AL}) and from experiment (ΔF_{exc}^{exp}).[22,57] Here we define the excess free energy as the free energy associated with the removal of a molecule from its own liquid. Thus, the sign is opposite from that used in the seminal works of Ben-Naim and Marcus.[57] The AL model underestimates ΔF_{exc} increasingly for larger chains (up to 15%). The CG model shows larger deviations from experiment, up to 32%. This is in line with the observed trends in the heat of vaporization. The intermolecular interaction, that is, interaction level III in the CG model,[1] underestimates the intermolecular attraction among oil particles.

 © 2007 Wiley-VCH Verlag GmbH & Co. KGaA, Weinheim

Table 2. Excess free energies (ΔF^{CG}_{exc} and ΔF^{AL}_{exc}) of hydrocarbon liquids (and corresponding errors) estimated via thermodynamic integration from CG ($r_1 = 0.0$ nm; $r_c = 1.4$ nm) and AL simulations at 303 K, and experimental values (ΔF^{exp}_{exc}) at 298 K. All values are in kJ mol^{-1}. See the Computational Methods section for details.

	C4	C8	C12	C16
ΔF^{CG}_{exc}	10.6 (0.5)	18.3 (1.1)	24.0 (1.4)	30.9 (1.4)
ΔF^{AL}_{exc}	7.4 (0.1)	21.7 (0.1)	26.8 (0.1)	38.5 (0.1)
$\Delta F^{exp\,[a]}_{exc}$	11.1	22.3	32.3	45.5

[a] Values at 298 K from Ben-Naim and Marcus.[57]

Figure 2 reports the free energies of solvating hydrocarbons in water from experiments (ΔF^{exp}_{hyd}) and from MD simulation at different model resolutions (ΔF^{CG}_{hyd} and ΔF^{AL}_{hyd}) and at different temperatures in the range between 263 and 343 K. The corresponding values are in Table S1 of the Supporting Information. For C4 and C8 at 303 K the AL force field provides values in agreement with experiment and with values previously reported[20] at 298 K. The values of ΔF^{CG}_{hyd} are too large, which means that the water/oil repulsion (i.e. interaction level V in the CG model[1]) is overestimated in the CG model. The ΔF^{CG}_{hyd} from the GROMACS and GROMOS05 treatments of nonbonded interaction differ by less than 2%. The variation of the hydration free energy with temperature shows a linear trend for both AL and CG models (the lowest linear regression coefficient is 0.96, observed for AL C4). The CG model shows a stronger dependence on temperature than the AL model. This indicates that the CG model displays less enthalpy–entropy compensation than the AL model, which may be due to the elimination of degrees of freedom upon coarse graining.

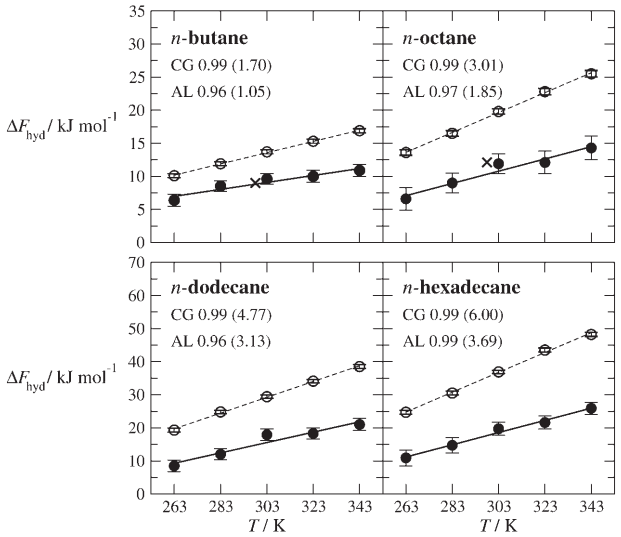

Figure 2. Hydration free energy (ΔF_{hyd}) as a function of the simulation reference temperature from CG (○) and AL (●) simulations of C4, C8, C12, and C16 in water with the GROMOS05 treatment of nonbonded interactions. The corresponding linear regression curves are also displayed (CG: – – –; AL: ——) together with their linear correlation coefficients (slopes in kJ mol^{-1} K^{-1}). Error bars are shown as vertical lines. Experimental values at 298 K are denoted by the symbol ×. See also Table S1.

In order to fully understand these trends, we calculated the change of solute–solvent interaction energy (ΔU_{UV}) upon hydration as a function of the simulation reference temperature from CG and AL simulations of C4, C8, C12, and C16 in water (Figure 3). As expected from the previous ΔF^{CG}_{hyd} values, ΔU^{CG}_{UV} values are not sufficiently negative compared to the ΔU^{AL}_{UV} ones. Both ΔU^{CG}_{UV} and ΔU^{AL}_{UV} values increase with increasing hydrocarbon chain length. As previously noticed from configurational entropy calculations,[32,33] the dependence of solute thermodynamic properties on changes in temperature is weaker for the CG model compared to the AL model, that is, CG models have a smaller heat capacity than AL ones, as a consequence of the reduced number of degrees of freedom.

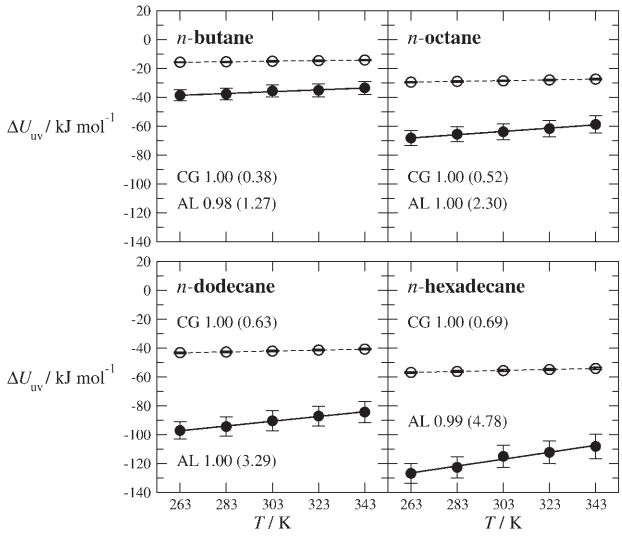

Figure 3. Solute–solvent interaction energy change upon hydration (ΔU_{uv}) as a function of the simulation reference temperature from CG (○, – – –) and AL (●, ——) simulations of the solutes C4, C8, C12, and C16 in water using the GROMOS05 treatment of nonbonded interactions. The corresponding linear regression curves are also displayed (CG: – – –; AL: ——) together with their linear correlation coefficients (slopes in kJ mol^{-1} K^{-1}). Error bars are shown as vertical lines. See also Table S2.

Figure 4 shows the solute/solvent entropy change (ΔS_{UV}) upon hydration as a function of the simulation reference temperature. The ΔS^{CG}_{UV} values are not sufficiently negative compared to ΔS^{AL}_{UV} values. Combining the ΔU_{UV} and the $-T\Delta S_{UV}$ values for both AL and CG models, the weaker dependence of ΔF^{AL}_{hyd} on T compared to ΔF^{CG}_{hyd} (Figure 2) is due to the stronger enthalpy–entropy compensation in the AL model.

We also estimate the solvent–solvent entropy changes ΔS^{CG}_{vv} and ΔS^{AL}_{vv} upon hydrating C4, C8, C12, and C16 hydrocarbons (i.e. the solvent reorganization entropy; see Computational Methods). As previously reported, these quantities are difficult to converge.[23,58,59] We find considerable error bars on these quantities at both resolutions (see Figure S2 in the Supporting Information).

 © 2007 Wiley-VCH Verlag GmbH & Co. KGaA, Weinheim

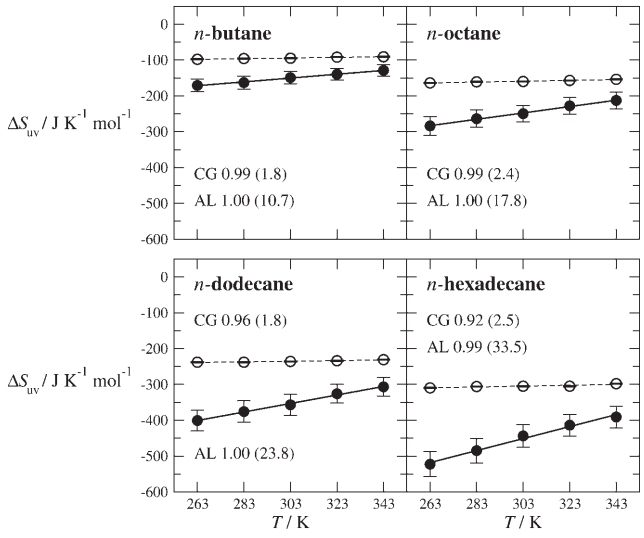

Figure 4. Solute–solvent entropy change upon hydration (ΔS_{uv}) as a function of the simulation reference temperature from CG (○) and AL (●) simulations of the solutes C4, C8, C12, and C16 in water using the GROMOS05 treatment of nonbonded interactions. The corresponding linear regression curves are also displayed (CG: – – –; AL: ——) together with their linear correlation coefficients (slopes in $J K^{-2} mol^{-1}$). Error bars are shown as vertical lines. See also Table S3.

Solvation Free Energies of Water at CG and AL Resolutions

The solvation properties of the CG water model are studied in terms of its excess free energy (ΔF^{CG}_{exc}) as calculated from TI in the range between 263 and 343 K. This is equivalent to the solvation of a CG water bead in its own liquid, but with opposite sign. An experimental value ΔF^{exp}_{exc} of 24.0 kJ mol^{-1} at 298 K has been reported.[60] A ΔF^{AL}_{exc} value of 23.3 ± 0.6 kJ mol^{-1} was calculated for the SPC (AL) water model.[61] At 303 K we obtain a ΔF^{CG}_{exc} value of 17.9 ± 0.4 kJ mol^{-1} (a similar value of 16.9 ± 1.0 kJ mol^{-1} was estimated using the GROMACS treatment of the nonbonded interactions). We note, however, that ΔF^{CG}_{exc} values should be compared to the corresponding excess free energy of a water tetramer. We find an excess free energy of 22.0 ± 0.6 kJ mol^{-1} for the insertion of an SPC water tetramer into SPC water, and of 19.2 ± 0.7 kJ mol^{-1} for the insertion of an SPC water tetramer into a liquid of SPC tetramers. The ΔF^{CG}_{exc} value compares well to this value, which indicates that the insertion of a CG water bead into its liquid is reasonably well represented by the CG water model. Values of ΔF^{CG}_{exc} in the temperature range between 263 and 343 K are shown in Figure 5. They decrease upon increasing the simulation temperature. We note that the experimental temperature dependence has a comparable slope of about -0.05 kJ mol^{-1} K^{-1} (Figure 2.18 in ref. [22]). Additionally, Figure 5 displays the change in solute–solvent interaction energy upon hydration of CG water (ΔU_{UV}) and the corresponding solute–solvent entropy change upon hydration (ΔS_{UV}). Both quantities decrease upon increasing the temperature.

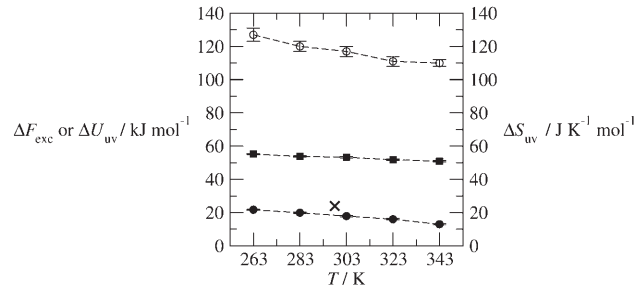

Figure 5. Helmholtz excess free energies of CG water (ΔF^{CG}_{exc}; ●), and corresponding solvent–solute interaction energy change (ΔU^{CG}_{uv}; ■), and solute-solvent entropy change (ΔS^{CG}_{uv}; ○) as a function of the simulation reference temperature. Error bars are shown as vertical lines. The experimental ΔF^{exp}_{exc} value at 298 K is denoted by the symbol ×.

Water/Oil Partitioning in the CG Model

Partitioning thermodynamics are also investigated. ΔF^{CG}_{solv} values are calculated at 303 K for the insertion of a CG water bead into liquids of aliphatic hydrocarbons of increasing chain length. We find ΔF^{CG}_{solv} values of C4: 4.1 ± 0.4, C8: 6.6 ± 0.5, C12: 8.0 ± 0.6, and C16: 8.8 ± 0.8 kJ mol^{-1} using the GROMOS05 treatment of nonbonded interactions (values within 1% are found using the GROMACS treatment of nonbonded interactions). This yields $\Delta\Delta F_{w/o}$ values for partitioning of water in water and water in hydrocarbon at 303 K of C4: 22.0, C8: 24.5, C12: 25.9, and C16: 26.7 kJ mol^{-1} [Eq. (9)]. The latter value agrees well with the experimental value[62] of 25 kJ mol^{-1}. Corresponding free energies $\Delta\Delta F_{w/o}$ for partitioning of hydrocarbon in hydrocarbon and hydrocarbon in water were also calculated [Eq. (10)] at 303 K C4: 24.3, C8: 38.1, C12: 53.4, and C16: 67.8 kJ mol^{-1}. The experimental $\Delta\Delta F^{exp}_{o/w}$ value for C16 is larger than 50 kJ mol^{-1}.[1,62–65]

Computational Methods

Molecular Dynamics Simulations: Trajectories for (CG or AL) hydrocarbon molecules (*n*-butane: C4; *n*-octane: C8; *n*-dodecane: C12; *n*-hexadecane: C16) and CG[1] or SPC[66] water (wt) were generated by using the GROMOS05 package of programs[53] and the GROMACS package of programs.[52] The CG force field is that proposed by Marrink et al.[1] with a slight modification when using the GROMOS05 software (see Appendix), and the AL model is the GROMOS96 45A3 one.[16,20] CG alkanes were solvated in approximately 400 CG wt beads (i.e. C4: 399, C8: 398, C12: 397, C16: 396) and were simulated in rectangular boxes using periodic boundary conditions. AL alkanes were solvated in boxes of large volumes (i.e. containing C4: 1151, C8: 2051, C12: 2077, C16: 2720 water molecules). Simulations of the corresponding pure liquids were performed at both CG (wt: 400, C4: 400, C8: 200, C12: 100, C16: 100 molecules) and AL (wt: 1600, C4: 1600, C8: 2059, C12: 2080, C16: 2721) model resolutions in order to study vaporization thermodynamics, diffusion, and properties of their liquid structures.

The temperature (values reported in the Results and Discussion section) and pressure (1 atm) were kept constant by using a weak-coupling algorithm[67] (relaxation times of 0.1 and 0.5 ps, respectively). Identical experimental values for CG and AL simulations have been set for the isothermal compressibility κ_T when using pressure coupling [wt: 0.75, C4: 5.0, C8: 1.6, C12: 1.6, C16: 1.6×10^{-2} (kJ mol^{-1} nm^{-3})$^{-1}$]. When calculating the (Helmholtz) free energies, the volume was kept constant instead of the pressure. All MD simulations were initialized with i) particle positions reproducing

 © 2007 Wiley-VCH Verlag GmbH & Co. KGaA, Weinheim

experimental liquid densities and ii) velocities taken from a Maxwell–Boltzmann distribution at the corresponding temperature. Newton's equations of motion were integrated using the leapfrog algorithm[68] with a time step of 20 fs (CG) or 2 fs (AL). For AL systems the simulation protocol is identical to that previously reported for its parameterization.[20]

In CG simulations, a number of changes are made in the simulation protocol. Bond-length constraining was not employed. Nonbonded interactions between second-nearest neighbors were not excluded. Nonbonded interactions were updated every time step. In the GROMOS05 simulations, the van der Waals potential energy term was smoothly shifted to zero between a distance of $r_1 = 0.0$ nm and its cutoff distance of $r_c = 1.4$ nm. The original CG model[1] made use of a different switching function implemented in the GROMACS program,[52] starting the switching at 0.9 nm, and using a cutoff of 1.2 nm. The differences between the GROMOS05 and GROMACS non-bonded energy terms are discussed in the Appendix at the end of this article.

Enthalpy of Vaporization: The enthalpy of vaporization ΔH_{vap} was estimated from two simulations, one for the liquid phase and a second for the gas phase, as previously described.[19,20] The (*N,V,T*) simulations of the hydrocarbon systems were equilibrated for 1.5 ns up to 6 ns, until the average pressure converged. The final configurations and velocities of these liquid hydrocarbon systems were used to generate initial positions and velocities for the gas-phase simulations. Each individual molecule was then simulated without intermolecular interactions in the gas phase at 303 K. Vaporization enthalpies were calculated as the difference between the (per molecule) potential energy in the gas phase and in the liquid phase plus an *RT* term. Corresponding errors were determined from the two standard deviations from the average.

Calculation of Excess Free Energy: The excess Helmholtz free energy ΔF_{exc} of the liquid hydrocarbons and of liquid water at 303 K at both CG and AL resolutions were calculated using standard thermodynamic integration techniques.[69] The system was perturbed from the liquid state (A, $\lambda = 1$) to the gas state (B, $\lambda = 0$) by progressively removing, as a function of λ, the intermolecular interactions in (*N,V,T*) simulations which were performed for 50 (CG) or 25 (AL) intermediate λ values. For each individual λ value at least 3 ns (CG) or 0.2 ns (AL) for equilibration and at least 6 ns (CG) or 0.2 ns (AL) were used for analysis. Additional sampling [up to 15 ns (CG) or 6 ns (AL)] was required for particular λ values. The integration procedure and calculation of the corresponding errors were as described in ref. [70]. A value $\alpha_{LJ} = 0.7$ for the soft-core parameter[71] was chosen for both CG and AL models.

Calculation of Solvation Free Energy: The free energy change between two states A and B of a molecular system was estimated by using the thermodynamic integration (TI) procedure [Eq. (1)][37,46]

$$\Delta F_{BA} = F_B - F_A = \int_{\lambda_A}^{\lambda_B} d\lambda \left\langle \frac{\partial U_{UV}(\lambda)}{\partial \lambda} \right\rangle_\lambda \quad (1)$$

where $U_{UV}(\lambda)$ denotes the potential energy function describing the total solute–solvent interaction, the average $\langle \ldots \rangle_\lambda$ is taken over the MD trajectory, and λ is a coupling parameter that regulates the strength of U_{UV} and varies linearly from full ($\lambda = 0$) to zero ($\lambda = 1$) interaction. It is assumed that only the solute–solvent interaction U_{UV} in the Hamiltonian *H* depends on λ. Simulations were performed at constant volume for 50 (CG) or 25 (AL) intermediate λ values until a smooth curve for the free energy derivative was obtained (see Figure S1 in the Supporting Information), which was then integrated numerically (i.e. by trapezoidal integration). The free energy of the compounds in vacuum were estimated from analogous runs, as previously described.[72] For each individual λ value at least 3 ns (CG) or 0.2 ns (AL) for equilibration and at least 6 ns (CG) or 0.2 ns (AL) were used for analysis. Additional sampling [up to 15 ns (CG) or 12 ns (AL)] was required for particular λ values, especially at 263 K. Free energies of solvation are reported for i) hydrocarbons in water (i.e. the hydration free energies ΔF_{hyd}^{CG} and ΔF_{hyd}^{AL}), ii) CG water in CG hydrocarbon liquids (i.e. the solvation free energy ΔF_{solv}^{CG}). The length of each simulation was varied in order to obtain converged averages. Soft-core solute–solvent interactions were used with a soft-core parameter[16] $\alpha_{LJ} = 0.7$ (CG) or 0.5 (AL) to avoid singularities of the free energy when annihilating ($\lambda \rightarrow 1$) interaction sites.[71]

Calculation of Entropy of Solvation: The change in entropy upon solvation was also analyzed.[58,59] This quantity is the sum of two contributions: one coming from the solute–solvent interaction and another from the solvent–solvent interaction, often referred to as the solvent reorganization term [Eqs. (2)–(7)]

$$\Delta S_S = \Delta S_{uv} + \Delta S_{vv} \quad (2)$$

with the terms ΔS_{uv} and ΔS_{vv} defined in Equations (3) and (4) respectively,

$$\Delta S_{uv} = \frac{1}{kT^2} \int_0^1 d\lambda \left[\langle U_{uv}(\lambda) \rangle_\lambda \left\langle \frac{\partial}{\partial \lambda} U_{uv}(\lambda) \right\rangle_\lambda - \left\langle U_{uv}(\lambda) \frac{\partial}{\partial \lambda} U_{uv}(\lambda) \right\rangle_\lambda \right] \quad (3)$$

$$\Delta S_{vv} = \frac{1}{kT^2} \int_0^1 d\lambda \left[\langle U_{vv}(\lambda) \rangle_\lambda \left\langle \frac{\partial}{\partial \lambda} U_{uv}(\lambda) \right\rangle_\lambda - \left\langle U_{vv}(\lambda) \frac{\partial}{\partial \lambda} U_{uv}(\lambda) \right\rangle_\lambda \right] \quad (4)$$

and ΔU_S is [Eq. (5)]

$$\Delta U_S = \Delta U_{uv} + \Delta U_{vv} \quad (5)$$

with ΔU_{uv} and ΔU_{vv} defined by Equations (6) and (7)

$$\Delta U_{uv} = \langle U_{uv} \rangle_{\lambda=0} - \langle U_{uv} \rangle_{\lambda=1} \quad (6)$$

$$\Delta U_{vv} = T \Delta S_{vv}. \quad (7)$$

In principle, several approaches can be employed to obtain total entropy differences [Eq. (2)], but their practical application is not straightforward.[73] Although the solute–solvent contribution [Eq. (3)] converges quite rapidly, the solvent reorganization term [Eq. (4)] is quite difficult to calculate, since the averages are taken over all solvent–solvent interactions. However, the second term does not contribute directly to the free energy {it is cancelled by another term coming from the solvation energy [Eq. (7)]}.[23,58,59] Thus, it need only be calculated when solvation entropies are to be compared with experimental values. Similarly, the solute–solvent energy [Eq. (6)] converges reasonably quickly, but the total energy [Eq. (5)] is difficult to obtain due to the solvent reorganization [Eq. (7)].

An alternative method to obtain the total entropy change upon hydration (or solvation in general) is by calculating finite differences[50] of the free energy at different temperatures. In this approach, it is assumed that the heat capacity C_p is constant in the considered $2\Delta T$ temperature range, so that [Eq. (8)]

$$\Delta S_S = -\frac{\partial G_{hyd}}{\partial T} \approx -\frac{\Delta G_{hyd}(T + \Delta T) - \Delta G_{hyd}(T - \Delta T)}{2\Delta T}. \quad (8)$$

 © 2007 Wiley-VCH Verlag GmbH & Co. KGaA, Weinheim

The assumption of constant C_p holds for the system considered in the present study, as can be inferred from results displayed in Figure 2.

Calculation of Partitioning Free Energy: The free energy of partitioning of water between the aqueous and the oil phases can be calculated using Equation (9)

$$\Delta\Delta F_{w/o} = \Delta F_{solv}(\text{water in oil}) + \Delta F_{exc}(\text{water}) \quad (9)$$

and the free energy of partitioning of oil between the aqueous and oil phases is given by Equation (10)

$$\Delta\Delta F_{o/w} = \Delta F_{hyd}(\text{oil in water}) + \Delta F_{exc}(\text{oil}) \quad (10)$$

We note that for a CG model i) the excess free energy of a pure liquid constituted by a single bead (wt and C4) is identical to the negative of its solvation free energy, and ii) for water its excess free energy is identical to the negative of its hydration free energy (the free energy in the gas phase is zero).

Analysis of Liquids: Radial distribution functions involving intermolecular particle distances were, after equilibration, calculated for C16 from 10^4 structures taken from 15 ns (CG) or 6 ns (AL) trajectories at 323 K. Self-diffusion coefficients (D) for both the CG and AL models were calculated from a least-squares fit to a straight line of the mean square displacements of all particles in the system as a function of time. In the text we refer to simulations of SPC tetramers. These were carried out as described above for AL MD simulations, but with additional use of a half-harmonic attractive restraining potential energy term among the SPC oxygen atoms of quadruples of water molecules. The restraining distance was set to 1.2 nm and a force constant of 500 kJ mol^{-1} nm^{-2} was employed. This keeps the 4 SPC water molecules within a sphere of 0.47 nm diameter, the average CG water–CG water bead distance, but simultaneously leaves rotational freedom to the SPC water molecules.

Treatment of Nonbonded Interactions in the CG Model Combined with Soft-Core Potentials: Figure 6 shows the soft-core Lennard–Jones potential energy term for the interaction of two CG water beads, as obtained from i) the GROMOS05 nonbonded potential energy term,[53] with force and energy smoothing at a cutoff distance of 1.4 nm, ii) the GROMOS05 soft-core potential energy term,[53] which simultaneously reproduces the soft-core character and the force and energy smoothing at a cutoff distance of 1.4 nm, and iii) the standard GROMOS96 soft-core potential energy term.[16] Only the GROMOS05 potential energy functions i) and ii) are smoothly shifted to zero at a cutoff distance of 1.4 nm with corresponding vanishing forces (see inset of Figure 6). Here we use the GROMOS05 soft-core form, that is, the force vanishes at the cutoff distance r_c for a shift function from $r_1 = 0.0$ nm and a cutoff distance of 1.4 nm. As discussed in the Appendix, the shape of this potential energy function is close to the one originally used for the parameterization of the CG force field[1] (Figure 7).

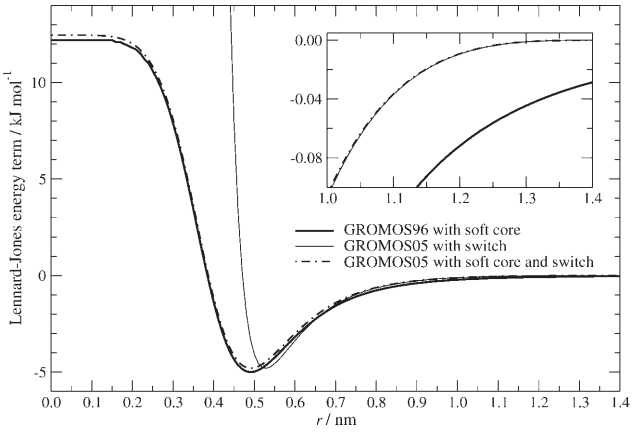

Figure 6. Comparison of Lennard–Jones potential energy terms for the interaction between two CG water beads[1] as a function of distance for the GROMOS05[53] form (——; with switch), the GROMOS05[53] form (–•–•; with soft core and switch), both used in this study, and the soft-core GROMOS96[16] form (——). The soft core parameter[16,71] is $\alpha_{LJ} = 0.7$. Switching is done over the range $r_1 = 0.0$ nm to $r_c = 1.4$ nm.

Conclusions

An analysis of vaporization, solvation, and water/oil partitioning thermodynamics is presented at two different levels of model resolution. These properties from a coarse-grained model were investigated by comparison with calculated atomic-level model properties and experimental data. The results at different model resolutions suggest that the coarse-grained force field investigated largely captures the physical properties of pure liquids and of solvation. However, there is ample room for improvement. A reparameterization based on the liquid-phase properties considered is likely to enhance the accuracy of the CG force field. In particular, oil/oil interactions are too weak, and water/oil repulsion is overestimated. The CG model displays less enthalpy–entropy compensation for solvation of alkanes in water than the AL model. The overall balance in the partitioning of the species is, however, reasonably well reproduced. The results confirm that the dependence of the thermodynamic quantities on the temperature is weaker for the CG force field compared to the AL one, due to a reduced number of degrees of freedom.

The present study suggests that accurate solvation thermodynamics could be employed as a solid physical basis for parameterizing and validating coarse-grained force fields, as has been done for well-established biomolecular atomic-level force fields.

Appendix

Here we discuss the Lennard–Jones (LJ) potential energy terms implemented as the GROMACS shift[74] and GROMOS05 switching[53] functions, respectively. The GROMACS shift function used in the parameterization of the coarse-grained (CG) model due to Marrink et al.[1] and the GROMOS05 switching function were used in this work to assess the thermodynamic properties of this model.

The GROMACS manuals (see http://www.gromacs.org) do not correctly describe the shift functions for arbitrary powers of $1/r$, which leads to incorrect expressions for the LJ energy terms. However, at least in GROMACS versions 2.0 through 3.2 the LJ force terms were correctly implemented. In this Appendix we wish to resolve any ambiguity and to clearly describe the potential energy terms used to parameterize the original CG model and the differences with respect to the GROMOS05 form also used in this work.

 © 2007 Wiley-VCH Verlag GmbH & Co. KGaA, Weinheim

The GROMACS User Manuals[52] (e.g., version 3.0, pp. 51–53) derive a form of the shift force $S_\alpha(r)$ to be added to forces of the form $r^{-(\alpha+1)}$ in order to let the force decay smoothly to zero at the cutoff distance r_c. The smooth decay may be initiated from a switching point r_1, with $0 \le r_1 < r_c$. Under the conditions that the forces and the first derivatives of the forces are i) continuous at r_1 and at r_c, and ii) zero at r_c, the simplest added force $S_\alpha(r)$ to be applied between r_1 and r_c, is a third-order polynomial given in the GROMACS manuals as Equation (A.1).

$$S_\alpha(r) = A(r-r_1)^2 + B(r-r_1)^3; \begin{cases} A = -\frac{(\alpha+4)r_c-(\alpha+1)r_1}{r_c^{(\alpha+2)}(r_c-r_1)^2} \\ B = \frac{(\alpha+3)r_c-(\alpha+1)r_1}{r_c^{(\alpha+2)}(r_c-r_1)^3} \end{cases} \quad \text{(A.1)}$$

It is here that the GROMACS manual is in error in that the definition of the shift force [Eq. (A.1)] is not general, but valid only for the modified Coulomb potential energy function ($\alpha = 1$), which is not explicitly stated in the manual. Such a wrongly documented potential energy term would lead to a discontinuity in the potential energy at the shift distance r_1 (Supporting Information, Figure S3). The mistake is triggered by the sentence "For pure Coulomb or Lennard–Jones interactions $F(r) = F_\alpha(r) = r^{-(\alpha+1)}$." In general, the force $F_\alpha(r) = \alpha r^{-(\alpha+1)}$. The modified LJ forces are sums of two forces with $\alpha = 6$ and $\alpha = 12$, respectively.

Integration of the negative of the force gives the potential energy. Note that a third boundary condition is introduced in the GROMACS manuals without stating it explicitly, that is, that iii) the potential energy be 0 at r_c. The expression given in the GROMACS manuals for the potential energy function is [Eq. (A.2)]

$$\Phi_\alpha(r) = \frac{1}{r^\alpha} - \frac{A}{3}(r-r_1)^3 - \frac{B}{4}(r-r_1)^4 - C; \quad C = \frac{1}{r_c^\alpha} - \frac{A}{3}(r_c-r_1)^3 - \frac{B}{4}(r_c-r_1)^4. \quad \text{(A.2)}$$

The correct expression should be [Eq. (A.3)]

$$\Phi_\alpha(r) = \frac{1}{r^\alpha} - \frac{\alpha A}{3}(r-r_1)^3 - \frac{\alpha B}{4}(r-r_1)^4 - C; \quad C = \frac{1}{r_c^\alpha} - \frac{\alpha A}{3}(r_c-r_1)^3 - \frac{\alpha B}{4}(r_c-r_1)^4. \quad \text{(A.3)}$$

Christen et al.[53] derived an additive switching function for use in GROMOS05. They start from the form of the potential energy [Eq. (A.4)]

$$S_\alpha(r) = -\frac{A}{3}(r-r_1)^3 - \frac{B}{4}(r-r_1)^4 - C; r_1 \le r \le r_c \quad \text{(A.4)}$$

rather than of the force, denoting the potential energy switching function by $S_\alpha(r)$, the same notation as used for the force shift function in the GROMACS manuals. The resulting potential energy function is exactly the same as the form given above [Eq. (A.3)]. By differentiating it, the force switching function $S_\alpha(r)$ contains a factor α compared to the force shift function [Eq. (A.2)] given in the GROMACS manual [Eq. (A.5), cf. Eq. (A.1)]

$$S'_\alpha(r) = -A(r-r_1)^2 - B(r-r_1)^3; \begin{cases} A = \frac{\alpha\{(\alpha+1)r_1-(\alpha+4)r_c\}}{r_c^{(\alpha+2)}(r_c-r_1)^2} \\ B = -\frac{\alpha\{(\alpha+1)r_1-(\alpha+3)r_c\}}{r_c^{(\alpha+2)}(r_c-r_1)^3} \end{cases} \quad \text{(A.5)}$$

and Equation (A.6)

$$C = \frac{1}{r_c^\alpha} - \frac{A}{3}(r_c-r_1)^3 - \frac{B}{4}(r_c-r_1)^4; r_1 \le r \le r_c \quad \text{(A.6)}$$

is chosen such that the potential energy is zero for $r = r_c$. The GROMACS[52] shift functions (A.2) and (A.3) are therefore identical to the GROMOS05[53] switching function for the Coulomb forces, but the GROMACS shift function (A.2) is different for the LJ interaction. Moreover, we note that both the GROMACS and GROMOS05 shift functions, Equations (A.3) and (A.4)–(A.6), have a discontinuity in the energy at $r = r_1$ of size $-C$.

Although the shift functions for force and potential given in the GROMACS manuals are not correct (see Figure S3) for the LJ terms, they have been implemented correctly in the code[75] for the case $r_1 = 0$. In the case $r_1 > 0$, the force was correctly implemented, but the potential energy term was not. The constant shift term C is applied over the entire range of the potential energy function, that is, also when $r \le r_1$. This removes the discontinuity in the potential energy at $r = r_1$. Again, this is not stated anywhere in the description of the shift function,[74] but is implemented in the code.[75] In GROMOS05 the potential energy is correctly implemented, that is, with the discontinuity at $r = r_1$. For $r_1 = 0$, there is no discontinuity. The parameters developed for the CG model are therefore not transferable between the GROMACS and GROMOS05 functions in the case $r_1 \neq 0$. However, using the original CG model parameters with $r_c = 1.4$ nm instead of $r_c = 1.2$ nm in combination with the GROMOS05 shift function with $r_1 = 0$ constitutes a good approximation of the original CG model with $r_c = 1.2$ nm, $r_1 = 0.9$ nm and the GROMACS function.

As an example, the combined LJ terms for interaction between two CG water beads[1] (type P, interaction level I, $C_6 = 4\varepsilon\sigma^6 = 4 \times 5.0 \times 0.47^6 = 0.21558$ kJ mol^{-1} nm^6; $C_{12} = 4\varepsilon\sigma^{12} = 2.3238 \times 10^{-3}$ kJ mol^{-1} nm^{12}) are shown in Figure 7, using either the shifting function (switching the force from $r_1 = 0.9$ nm, with $r_c = 1.2$ nm) as was used in the parameterization of the CG force field,[1] or the shifting function (smoothing of the force from $r_1 = 0.0$ nm, with $r_c = 1.2$ nm) as is used in the GROMOS05 implementation of the shift function. The LJ interaction using the shifting function switching the force smoothly from $r_1 = 0.0$ nm, with $r_c = 1.4$ nm, which is the one used in this work, is shown in Figure 7 as well. It is seen that the GROMOS05 potential energy function with $r_1 = 0.0$ nm and $r_c = 1.4$ nm is closer to the GROMACS potential energy function with $r_1 = 0.9$ nm and $r_c = 1.2$ nm than the GROMOS05 potential energy function with $r_1 = 0.0$ nm and $r_c = 1.2$ nm. This is why in this study a value of $r_c = 1.4$ nm was used in combination with the GROMOS05 function ($r_1 = 0.0$ nm) and the original CG model parameters.

 © 2007 Wiley-VCH Verlag GmbH & Co. KGaA, Weinheim

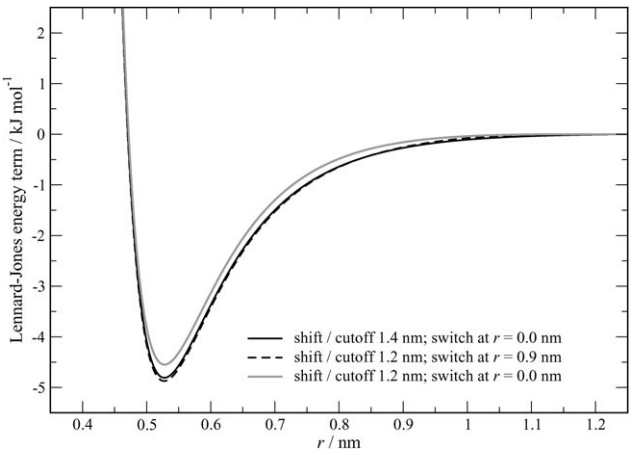

Figure 7. Lennard-Jones pontential energy functions with different switching ranges. The interaction between two CG water beads[1] is shown as an example: force shifted from switching point $r_1 = 0.0$ nm, cutoff $r_c = 1.4$ nm (——); force shifted from switching point $r_1 = 0.9$ nm, cutoff $r_c = 1.2$ nm (-----) as used in the parameterization of the CG force field;[1] force shifted from switching point $r_1 = 0.0$ nm; cutoff $r_c = 1.2$ nm (——). The latter function was not used in the present work.

Acknowledgements

Financial support from the National Center of Competence in Research (NCCR) Structural Biology of the Swiss National Science Foundation (SNSF) is gratefully acknowledged. The authors thank Dr. Markus Christen for insightful discussions.

Keywords: computational chemistry · energy–entropy compensation · force field · GROMOS · GROMACS

[1] S. J. Marrink, A. H. de Vries, A. E. Mark, *J. Phys. Chem. B* **2004**, *108*, 750.
[2] J. Baschnagel, K. Binder, P. Doruker, A. A. Gusev, O. Hahn, K. Kremer, W. L. Mattice, F. Müller-Plathe, M. Murat, W. Paul, S. Santos, U. W. Suter, V. Tries in *Viscoelasticity, Atomistic Models, Statistical Chemistry, Vol 152,* Advances in Polymer Sciences, Springer, Heidelberg, **2000**, pp. 41 – 165.
[3] F. Müller-Plathe, *ChemPhysChem* **2002**, *3*, 754.
[4] K. Kremer, *Macromol. Chem. Phys.* **2003**, *204*, 257.
[5] B. Smit, P. A. J. Hilbers, K. Esselink, L. A. M. Rupert, N. M. van Os, A. G. Schlijper, *Nature* **1990**, *348*, 624.
[6] R. Goetz, R. Lipowsky, *J. Chem. Phys.* **1998**, *108*, 7397.
[7] R. D. Groot, T. J. Madden, D. J. J. Tildesley, *J. Chem. Phys.* **1999**, *110*, 9739.
[8] J. C. Shelley, M. Y. Shelley, R. C. Reeder, S. Bandyopadhyay, M. L. Klein, *J. Phys. Chem. B* **2001**, *105*, 4464.
[9] M. Müller, K. Katsov, M. Schick, *J. Polym. Sci.* **2003**, *41*, 1441.
[10] S. Izvekov, G. A. Voth, *J. Chem. Theory Comput.* **2006**, *2*, 637
[11] J. C. Shillcock, R. Lipowsky, *J. Phys. Condens. Matter* **2006**, *18*, S1191.
[12] V. Tozzini, *Curr. Opin. Struct. Biol.* **2005**, *15*, 144.
[13] A. Y. Shih, A. Arkhipov, P. L. Freddolino, K. Schulten, *J. Phys. Chem. B* **2006**, *110*, 3674.
[14] P. J. Bond, M. S. P. Sansom, *J. Am. Chem. Soc.* **2006**, *128*, 2697.
[15] W. L. Jorgensen, D. S. Maxwell, J. Tirado-Rives, *J. Am. Chem. Soc.* **1996**, *118*, 11225.
[16] W. F. van Gunsteren, S. R. Billeter, A. A. Eising, P. H. Hünenberger, P. Krüger, A. E. Mark, W. R. P. Scott, I. G. Tironi, *Biomolecular Simulation: The GROMOS96 Manual and User Guide*, vdf Hochschulverlag AG an der ETH Zürich and BIOMOS b.v., Zürich, Groningen, **1996**.
[17] D. A. Case, T. E. Cheatham, T. Darden, H. Gohlke, R. Luo, K. M. Merz, A. Onufriev, C. Simmerling, B. Wang, R. J. Woods, *J. Comput. Chem.* **2005**, *26*, 1668.
[18] W. F. van Gunsteren, X. Daura, A. E. Mark, *Encycl. Comput. Chem.* **1998**, *2*, 1211.
[19] X. Daura, A. E. Mark, W. F. van Gunsteren, *J. Comput. Chem.* **1998**, *19*, 535.
[20] L. D. Schuler, X. Daura, W. F. van Gunsteren, *J. Comput. Chem.* **2001**, *22*, 1205.
[21] C. Oostenbrink, A. Villa, A. E. Mark, W. F. van Gunsteren, *J. Comput. Chem.* **2004**, *25*, 1656.
[22] A. Ben-Naim, *Solvation Thermodynamics*, Plenum, New York, **1987**.
[23] N. F. A. van der Vegt, W. F. van Gunsteren, *J. Phys. Chem. B* **2004**, *108*, 1056.
[24] D. Trzesniak, N. F. A. van der Vegt, W. F. van Gunsteren, *Phys. Chem. Chem. Phys.* **2004**, *6*, 697.
[25] G. Graziano, *J. Phys. Chem. B* **2005**, *109*, 12160.
[26] N. S. Bodor, Z. Gabanyi, C.-K. Wong, *J. Am. Chem. Soc.* **1989**, *111*, 3783.
[27] M. J. Warne, D. W. Connell, D. W. Hawker, G. Schueuermann, *Chemosphere* **1989**, *19*, 1113.
[28] G. J. Niemi, S. C. Basak, G. D. Veith, G. Grunwald, *Environ. Toxicol. Chem.* **1992**, *11*, 893.
[29] R. Faller, S. J. Marrink, *Langmuir* **2004**, *20*, 7686.
[30] S. J. Marrink, A. E. Mark, *Biophys. J.* **2004**, *87*, 3894.
[31] S. J. Marrink, J. Risselada, A. E. Mark, *Chem. Phys. Lipids* **2005**, *135*, 223.
[32] R. Baron, A. H. de Vries, P. H. Hünenberger, W. F. van Gunsteren, *J. Phys. Chem. B* **2006**, *110*, 15602.
[33] R. Baron, A. H. de Vries, P. H. Hünenberger, W. F. van Gunsteren, *J. Phys. Chem. B* **2006**, *110*, 8464.
[34] F. Reif in *Fundamentals of Statistical and Thermal Physics*, McGraw-Hill, Singapore, **1985**, pp. 312 – 315.
[35] J. W. Essex, C. A. Reynolds, W. G. Richards, *J. Chem. Soc. Chem. Commun.* **1989**, 1152.
[36] W. L. Jorgensen, J. M. Briggs, M. L. Contreras, *J. Phys. Chem.* **1990**, *94*, 1683.
[37] D. L. Beveridge, F. M. DiCapua, *Annu. Rev. Biophys. Biophys. Chem.* **1989**, *18*, 431.
[38] T. P. Straatsma, J. A. McCammon, *Annu. Rev. Phys. Chem.* **1992**, *43*, 407.
[39] P. M. King in *Computer Simulation of Biomolecular Systems, Theoretical and Experimental Applications, Vol. 2* (Eds.: W. F. van Gunsteren, P. K. Weiner, A. J. Wilkinson), Escom, Leiden, **1993**, pp. 267 – 314.
[40] P. Kollman, *Chem. Rev.* **1993**, *93*, 2395.
[41] W. F. van Gunsteren, T. C. Beutler, F. Fraternali, P. M. King, A. E. Mark, P. E. Smith in *Computer Simulation of Biomolecular Systems, Theoretical and Experimental Applications, Vol. 2* (Eds.: W. F. van Gunsteren, P. K. Weiner, A. J. Wilkinson), Escom, Leiden, **1993**, pp. 315 – 348.
[42] T. P. Straatsma in *Reviews in Computational Chemistry, Vol. 9* (Eds.: K. B. Lipkowitz, D. B. Boyd), VCH, New York, **1996**, pp. 81 – 127.
[43] A. E. Mark, *Encycl. Comput. Chem.* **1998**, *2*, 1070.
[44] W. P. Reinhardt, M. A. Miller, L. M. Amon, *Acc. Chem. Res.* **2001**, *34*, 607.
[45] C. Chipot, D. A. Pearlman, *Mol. Simul.* **2002**, *28*, 1.
[46] W. F. van Gunsteren, X. Daura, A. E. Mark, *Helv. Chim. Acta* **2002**, *85*, 3113.
[47] B. Widom, *J. Chem. Phys.* **1963**, *39*, 2808.
[48] B. Guillot, Y. Guissani, S. Bratos, *J. Chem. Phys.* **1991**, *95*, 3643.
[49] B. Guillot, Y. Guissani, *J. Chem. Phys.* **1993**, *99*, 8075.
[50] S. H. Fleischman, C. L. Brooks, *J. Chem. Phys.* **1987**, *87*, 3029.
[51] W. F. van Gunsteren, D. Bakowies, R. Baron, I. Chandrasekhar, M. Christen, X. Daura, P. Gee, D. P. Geerke, A. Glättli, P. H. Hünenberger, M. A. Kastenholz, C. Oostenbrink, M. Schenk, D. Trzesniak, N. F. A. van der Vegt, H. B. Yu, *Angew. Chem.* **2006**, *118*, 4168 – 4198; *Angew. Chem. Int. Ed.* **2006**, *45*, 4064 – 4092.
[52] D. van der Spoel, A. R. van Buuren, M. E. F. Apol, P. J. Meulenhoff, D. P. Tieleman, A. L. T. M. Sijbers, B. Hess, K. A. Feenstra, E. Lindahl, R. van Drunen, H. J. C. Berendsen, *GROMACS User Manual version 3.1.1*, Nijenborgh 4, 9747 AG Groningen, The Netherlands, **2001**. Internet: http://www.gromacs.org/.
[53] M. Christen, P. H. Hünenberger, D. Bakowies, R. Baron, R. Bürgi, D. P. Geerke, T. N. Heinz, M. A. Kastenholz, V. Kräutler, C. Oostenbrink, C. Peter, D. Trzesniak, W. F. van Gunsteren, *J. Comput. Chem.* **2005**, *26*, 1719.
[54] D. R. Lide, *CRC Handbook of Chemistry and Physics*, 72nd ed., CRC, Boca Raton, **1992**.

 © 2007 Wiley-VCH Verlag GmbH & Co. KGaA, Weinheim

[55] K. Krynicki, C. D. Green, D. W. Sawyer, *Faraday Discuss. Chem. Soc.* **1978**, *66*, 199.
[56] D. C. Douglass, D. W. Mccall, *J. Phys. Chem.* **1958**, *62*, 1102.
[57] A. Ben-Naim, Y. Marcus, *J. Chem. Phys.* **1984**, *81*, 2016.
[58] H.-A. Yu, M. Karplus, *J. Chem. Phys.* **1988**, *89*, 2366.
[59] N. F. A. van der Vegt, D. Trzesniak, B. Kasumaj, W. F. van Gunsteren, *ChemPhysChem* **2004**, *5*, 144.
[60] J. Hermans, A. Pathiaseril, A. Anderson, *J. Am. Chem. Soc.* **1988**, *110*, 5982.
[61] A. Glättli, X. Daura, W. F. van Gunsteren, *J. Comput. Chem.* **2003**, *24*, 1087.
[62] P. Schatzberg, *J. Phys. Chem.* **1963**, *67*, 776.
[63] *Vapour Pressures of Chemicals, Vol. 20* (Ed.: W. Martienssen) Landolt-Börnstein Series, Group IV, Springer, Darmstadt, **1999**.
[64] *IUPAC Solubility Data Series* (Ed.: J. W. Lorimer), Oxford University Press.
[65] For some compounds experimental ΔG^{exp}_{hyd} or ΔG^{exp}_{solv} values are not available in the literature. They can be calculated from the vapor pressure p_{vap} of the pure compound at 298 K and its molar concentration c_M in the solvent at saturated conditions as $\Delta G_{exp} = -kT \ln\left(\frac{p_{vap}}{p^{\phi} c_M}\right)$ where p^{ϕ} is the pressure of an ideal gas with concentration of 1 mol L^{-1}, i.e. $p^{\phi} = kT$.
[66] H. J. C. Berendsen, J. P. M. Postma, W. F. van Gunsteren, J. Hermans in *Intermolecular Forces* (Ed.: B. Pullman), D. Reidel Publishing Company, Dordrecht, **1981**, pp. 331 – 342.
[67] H. J. C. Berendsen, J. P. M. Postma, W. F. van Gunsteren, A. Di Nola, J. R. Haak, *J. Chem. Phys.* **1984**, *81*, 3684.
[68] R. W. Hockney, *Methods Comput. Phys.* **1970**, *9*, 136.
[69] I. G. Tironi, W. F. van Gunsteren, *Mol. Phys.* **1994**, *83*, 381.
[70] D. Fincham, N. Quirke, D. J. Tildesley, *J. Chem. Phys.* **1986**, *84*, 4535.
[71] T. C. Beutler, A. E. Mark, R. C. van Schaik, P. R. Gerber, W. F. van Gunsteren, *Chem. Phys. Lett.* **1994**, *222*, 529.
[72] A. Villa, A. E. Mark, *J. Comput. Chem.* **2002**, *23*, 548.
[73] C. Peter, C. Oostenbrink, A. van Dorp, W. F. van Gunsteren, *J. Chem. Phys.* **2004**, *120*, 2652.
[74] E. Lindahl, B. Hess, D. van der Spoel, *J. Mol. Model.* **2001**, *7*, 306.
[75] Using GROMACS versions 2.0 through to 3.2 the potentials and forces used in the codes are identical. Version 2.0 was used for the development of the CG force field.

Received: October 20, 2006

 © 2007 Wiley-VCH Verlag GmbH & Co. KGaA, Weinheim